PAPER

Helical flow in RFX-mod tokamak plasmas

IOP Publishing | International Atomic Energy Agency Nuclear Fusion

Nucl. Fusion **57** (2017) 056033 (13pp) https://doi.org/10.1088/1741-4326/aa5c5d

Helical flow in RFX-mod tokamak plasmas

L. Piron[1], B. Zaniol[2], D. Bonfiglio[2], L. Carraro[2], A. Kirk[1], L. Marrelli[2], R. Martin[1], C. Piron[2], P. Piovesan[2] and M. Zuin[2]

[1] CCFE, Culham Science Centre, Abingdon, OX14 3DB, United Kingdom
[2] Consorzio RFX (CNR, ENEA, INFN, Università di Padova, Acciaierie Venete SpA), Corso Stati Uniti 4, 35127 Padova, Italy

E-mail: lidia.piron@ukaea.uk

Received 10 October 2016, revised 20 December 2016
Accepted for publication 25 January 2017
Published 31 March 2017

Abstract

This work presents the first evidence of helical flow in RFX-mod $q(a) < 2$ tokamak plasmas. The flow pattern is characterized by the presence of convective cells with $m = 1$ and $n = 1$ periodicity in the poloidal and toroidal directions, respectively. A similar helical flow deformation has been observed in the same device when operated as a reversed field pinch (RFP). In RFP plasmas, the flow dynamic is tailored by the innermost resonant $m = 1$, $n = 7$ tearing mode, which sustains the magnetic field configuration through the dynamo mechanism (Bonomo *et al* 2011 *Nucl. Fusion* **51** 123007). By contrast, in the tokamak experiments presented here, it is strongly correlated with the $m = 1$, $n = 1$ MHD activity. A helical deformation of the flow pattern, associated with the deformation of the magnetic flux surfaces, is predicted by several codes, such as Specyl (Bonfiglio *et al* 2005 *Phys. Rev. Lett.* **94** 145001), PIXIE3D (Chacón *et al* 2008 *Phys. Plasmas* **15** 056103), NIMROD (King *et al* 2012 *Phys. Plasmas* **19** 055905) and M3D-C1 (Jardin *et al* 2015 *Phys. Rev. Lett.* **115** 215001). Among them, the 3D fully non-linear PIXIE3D has been used to calculate synthetic flow measurements, using a 2D flow modelling code. Inputs to the code are the PIXIE3D flow maps, the ion emission profiles as calculated by a 1D collisional radiative impurity transport code (Carraro *et al* 2000 *Plasma Phys. Control. Fusion* **42** 731) and a synthetic diagnostic with the same geometry installed in RFX-mod. Good agreement between the synthetic and the experimental flow behaviour has been obtained, confirming that the flow oscillations observed with the associated convective cells are a signature of helical flow.

Keywords: helical flow, plasma rotation, flow oscillations, PIXIE3D code

(Some figures may appear in colour only in the online journal)

1. Introduction

Plasma rotation in fusion devices can have a beneficial effect on plasma stability and confinement. For example, it is important to stabilize MHD modes, such as neoclassical tearing modes [1] and resistive wall modes (RWM) [2], it plays a role in reducing the error field penetration threshold and therefore enhances the plasma tolerance to error fields [3]. Moreover, a plasma rotation shear is a key factor for suppressing turbulence and forming transport barriers, which are important to achieve high-performance regimes [4]. In present day devices, a significant external momentum source can be provided by neutral beam injection (NBI). However, in ITER and future reactors, NBI is not expected to provide much momentum. Consequently, the study of the physical mechanisms that can influence plasma rotation is a topic of key importance in magnetic fusion research.

Three-dimensional (3D) magnetic fields can be present in fusion devices as intrinsic magnetic field errors, which arise inevitably because of imperfections or misalignment of the coils, 3D wall structures, and ferritic materials in the vicinity of the plasma. They can also be deliberately applied to control RWMs [5], edge localized modes [6], tearing modes (TM) [7], and to modify the edge transport [8] and suppress the runaway electrons [9].

Such 3D magnetic fields are known to affect plasma rotation [10]. In fact, they can brake the plasma via the electromagnetic torque that acts on magnetic islands [11–14]. In some

experiments, a local increase in the toroidal rotation in the pedestal region has been observed, due to the presence of a stochastic torque in the plasma edge [15, 16]. In other experiments, a global plasma braking can be associated with the neoclassical toroidal viscosity (NTV), resulting from the toroidal drag force experienced by the plasma particles moving along field lines distorted by 3D magnetic perturbations [17–19].

The RFX-mod experiment [20], when operated as a tokamak [5, 21–23], can contribute to the study of the effects responsible for momentum injection and transport in the absence of external heating systems, and of the impact of externally applied 3D magnetic fields on plasma rotation. The RFX-mod device is equipped with a sophisticated feedback control system, made up of 192 active coils, independently driven and fully covering the torus surface, which can induce a wide range of m/n 3D magnetic field perturbations (with m and n poloidal and toroidal mode numbers, respectively). Its feedback control system is capable of applying 3D magnetic fields in plasmas with both $q(a) < 2$ and $q(a) > 2$.

Recent RFX-mod tokamak experiments have shown that the application of 3D magnetic fields with 2/1 helicity in $q(a) < 2$ plasma regimes induces slowdown of plasma rotation for an applied radial magnetic field below a threshold value, whereas acceleration of rotation is induced for an applied field above the threshold value [24].

The novelty of the experiments reported in this paper is that, in the presence of rotating 3D magnetic fields, oscillations have been observed in the plasma flow, measured by the Doppler shift of spectral lines from several ion species. The flow oscillates at the same frequency as the MHD modes, i.e. the 2/1 RWM and the internal 1/1 kink mode, which are maintained into rotation by the magnetic feedback control system [5, 23]. By correlating flow measurements with radial magnetic field data, the presence of helical flow and $m = 1$, $n = 1$ convective cells has been inferred.

From a theoretical point of view, the helical magnetic structures correspond to a magnetohydrodynamic minimum energy state accessed through a bifurcation process, characterized by an internal 3D helical magnetic equilibrium [25], with the same helicity as the experimental perturbation. For example, in RFX-mod tokamak experiments, helical equilibria are associated with an internal 1/1 kink mode, which produces a helical distortion in the plasma core [26]. Conversely, in reversed field pinch (RFP) RFX-mod plasmas, helical equilibria are linked to the innermost resonant TM, which sustains the magnetic field configuration [27, 28].

The presence of an helical flow in tokamak plasmas has been predicted by several codes, such as Specyl [29], PIXIE3D [30], NIMROD [31] and M3D-C1 [32]. The origin of the helical flow can be described as follows. The helical distortion of the flux surfaces causes a modulation of the parallel current density. As a result, an electrostatic potential builds up to balance the finite, through a very small charge separation. Associated with this electrostatic potential, a helical flow is induced which produces a VxB dynamo electromotive force, sustaining the helical equilibrium [29, 33, 34].

Here, the signature of helical flow in the experimental data has been investigated. In particular, the 3D fully non-linear PIXIE3D code, which has been extensively validated against RFX-mod tokamak plasmas [24, 26, 35], has been used to interpret the origin of the observed flow oscillations in combination with ad-hoc 2D flow modelling code, which allows the reconstruction of rotation measurements. Inputs to the 2D flow modelling are the PIXIE3D flow map, the ion radial emission profiles as calculated by a 1D collisional radiative impurity transport code [36] and a synthetic passive spectroscopy diagnostic with the same geometry implemented in RFX-mod.

A good agreement has been obtained between the synthetic flow behaviour, calculated with the 2D flow modelling code, and the experimentally observed one, demonstrating that the flow oscillations observed with the associated convective cells are a signature of helical flow. This confirms that the dynamo and the associated helical flow can sustain helical equilibria not only in high current RFP plasmas [28, 37, 38], but also in low-β RFX-mod tokamak plasmas and high-β DIII-D hybrid tokamak operations [34, 39].

This paper is structured as follows: section 2 presents the interplay between toroidal rotation and MHD activity and the main dependence of the plasma rotation on magnetic equilibrium and electron density. Section 3 describes the evidence of toroidal and poloidal flow oscillations, and the associated convective cells, in the presence of externally applied magnetic field perturbations. Section 4 compares the results of the 2D flow modelling code with the experimental flow behaviour. Section 5 summarizes this work and draws conclusions.

2. Interplay between toroidal rotation and MHD activity

The RFX-mod device has been operated as a circular tokamak, exploring magnetic equilibria with $q(a) < 2$ and $q(a) > 2$ in various density regimes. The behaviour of plasma rotation in such experiments has been studied by use of data from a multichord Doppler spectroscopic diagnostic based on line of sight integrated emissivity measurements of various ion stages.

This diagnostic acquires the highly resolved spectra of selected impurity emission lines along several lines of sight (LOS). The geometry of the LOS in the toroidal and poloidal cross sections of RFX-mod is shown in figure 1 on the left and right, respectively. From the wavelength shift of the emission lines, it is possible to deduce the ion flow parallel to the LOS, using the Doppler formula. Coming from a LOS integrated signal, the ion flow measurement is not local but it is an averaged value that depends on the LOS geometry and on the impurity emission radial profiles.

Emissions from C VI, ($\lambda = 5290$ Å), the main impurity coming from the graphite first wall, and O V, ($\lambda = 6500$ Å), have been statistically characterized in standard Ohmic RFX-mod discharges, without external magnetic field perturbations. The mean radial location of the emitting ions must be known in order to derive the ion flow components. The reconstruction of the ion emissivity profiles is obtained by use of a 1D collisional radiative impurity transport code. The simulations have been performed for both coronal, no-transport regime, and high impurity transport regime characterized by

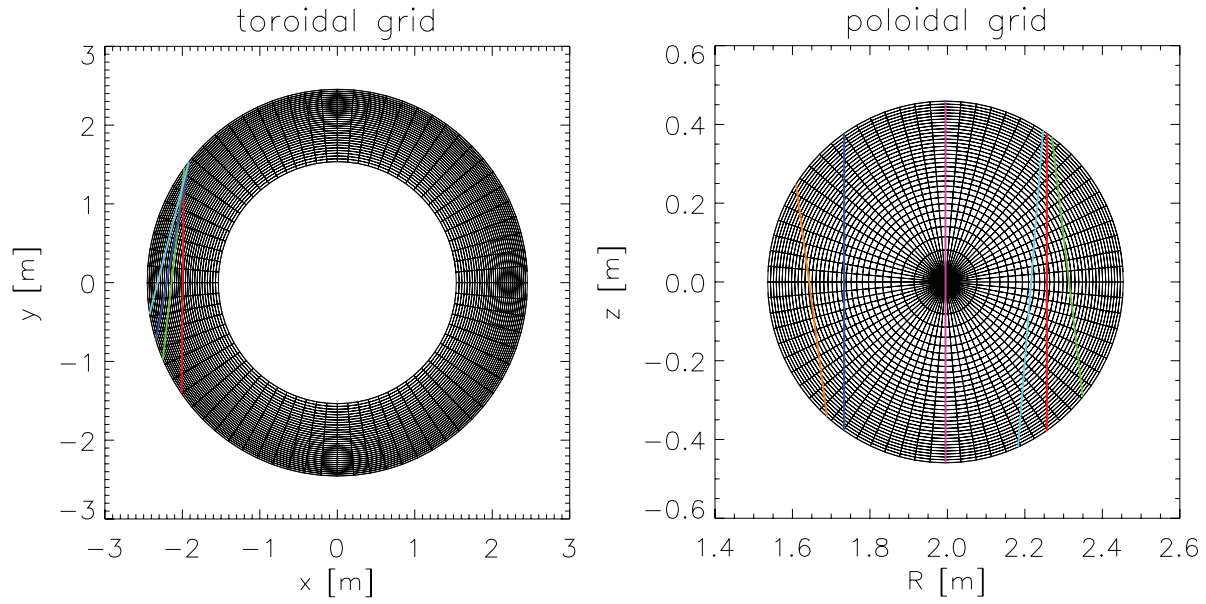

Figure 1. Toroidal (left) and poloidal (right) cross sections with fine grids and LOS geometry used in RFX-mod experiment and in the 2D flow modelling code, described in section 4.

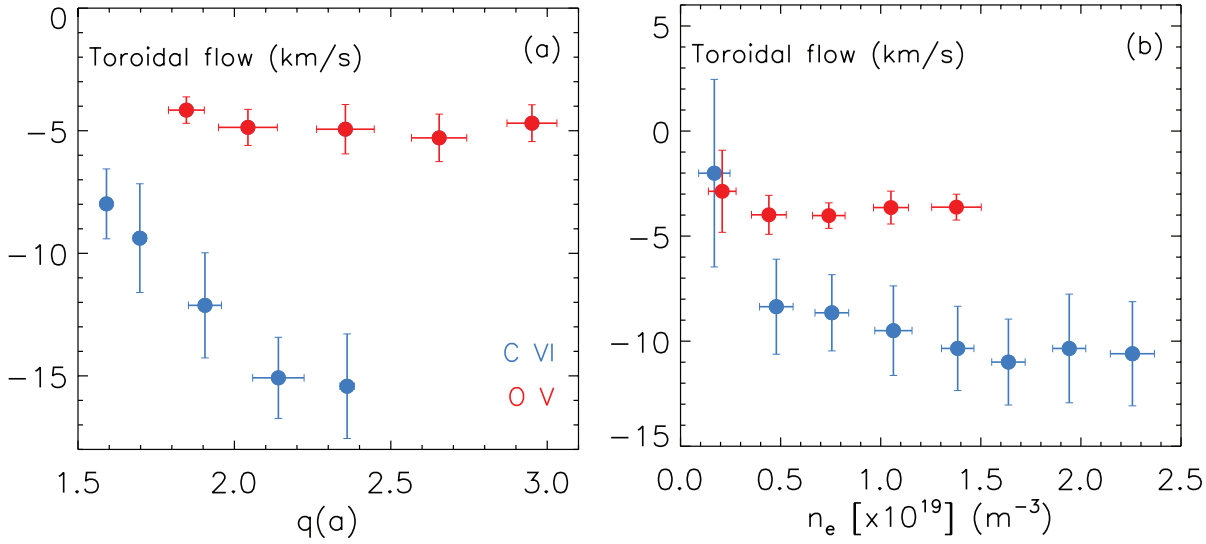

Figure 2. C VI toroidal flow (in blue), located at $r/a \approx 0.35$, and O V (in red), at $r/a \approx 0.8$, as a function of (*a*) edge safety factor and (*b*) electron plasma density. The location of ions emission has been calculated using a 1D collisional radiative code described in the text.

the transport coefficients $D = 20\ \mathrm{m^2\ s^{-1}}$ and v as in [36]. A scan on diffusion coefficient and pinch velocity in the impurity transport equations has shown that, independent of the hypothesis on the transport regime, the C VI emissivity is rather spread over the minor radius with a broad peak centred around mid radius, $r/a \approx 0.35$. In contrast, the O V emission is relatively sharply peaked near the edge, $r/a \approx 0.8$.

Toroidal rotation measurements from these ion emissions show that the intrinsic rotation in RFX-mod is strongly influenced by the edge safety factor, as reported in figure 2(*a*). This is similar to what has been observed in TCV Ohmic discharges [40]. Note that the intrinsic rotation in RFX-mod tokamak plasma is in counter-I_p direction (negative values). The rotation scaling results differ from those obtained in the Alcator C-mod experiment [41]; no velocity reversal occurs below a threshold value of plasma density, as highlighted in figure 2(*b*). In future RFX-mod experimental campaigns, the role of collisionality in producing the flow inversion [42] will be further investigated by dedicated experiments.

The poloidal flow component could be derived only from the intense line emission of C V ($\lambda = 2271$ Å), which is located around $r/a \approx 0.56$, as suggested by the 1D collisional radiative impurity transport code. It has low amplitudes, around $2\ \mathrm{km\ s^{-1}}$, likely due to neoclassical poloidal flow damping [43]. Unlike in the toroidal flow data, no correlations have been observed in poloidal rotation measurements varying the plasma parameters. Section 3 reports more details on poloidal flow in the presence of external 3D magnetic fields.

Interestingly, a significant change of toroidal plasma rotation has been observed in the presence of MHD modes. The following subsections present the plasma rotation behaviour in the presence of the 2/1 RWM and the 2/1 TM.

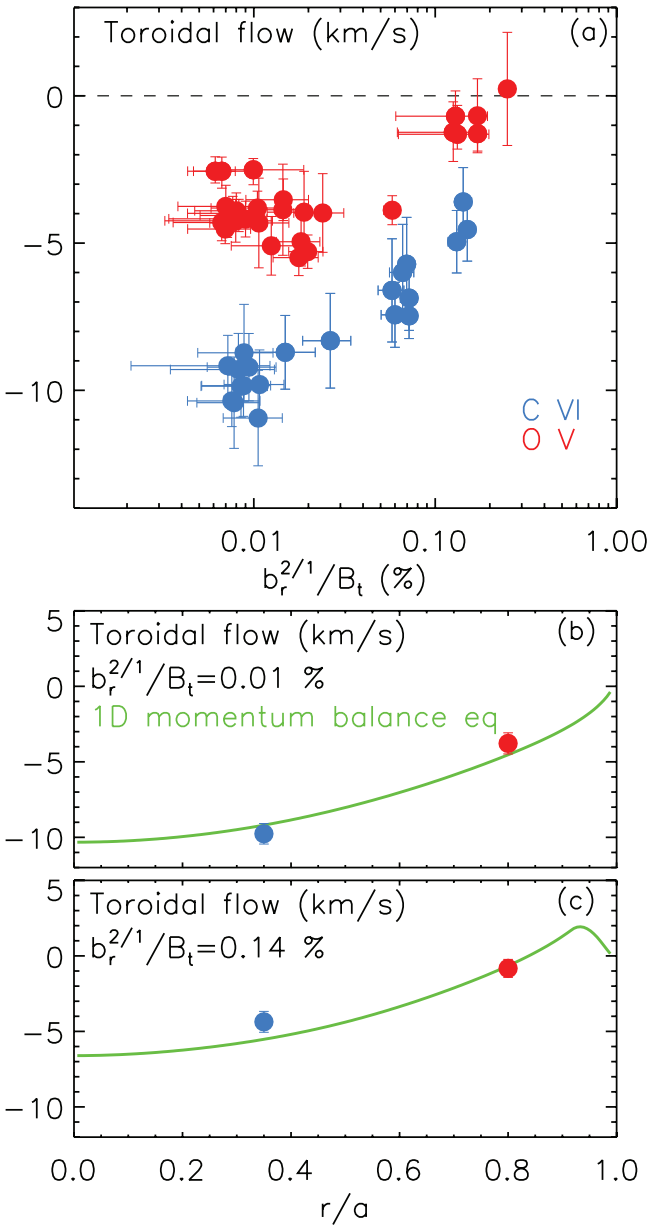

Figure 3. (*a*) Toroidal rotation as a function of $b_r^{2/1}/B_t$ for two sets of similar $q(a) < 2$ tokamak discharges. The blue dots correspond to data from C VI emission, the red ones to data from O V. (*c*)–(*d*) Radial profile of the toroidal rotation, solution of the 1D momentum transport model described in [24], in the absence of 2/1 magnetic field perturbations applied ($b_r^{2/1}/B_t \approx 0.01\%$) and in its presence ($b_r^{2/1}/B_t \approx 0.14\%$). The dots correspond to the mean value of rotation measurements from C VI and O V emission for the normalized 2/1 radial magnetic field amplitudes reported above. Reproduced courtesy of IAEA. Figure from [24]. Copyright 2013 IAEA.

2.1. Plasma rotation in the presence of 2/1 RWM

In RFX-mod $q(a) < 2$ tokamak plasmas, the 2/1 RWM can be controlled by the active feedback system, by zeroing the associated radial magnetic field, $b_r^{2/1}$, or can be kept at a finite amplitude by setting a finite reference value on the 2/1 radial magnetic field, which could be either rotated at a selected frequency or maintained static. In this work, the second technique has been applied to investigate the plasma rotation dynamics in the presence of a 2/1 RWM with a finite radial magnetic field amplitude.

Several experiments with similar plasma parameters have been performed by applying various amplitudes of the external 3D magnetic field, which rotates with 10 Hz frequency. The behaviour of toroidal rotation in these plasmas is reported in figure 3(*a*). The figure shows the C VI (blue) and O V (red) toroidal flow as a function of $b_r^{2/1}$ normalized to the toroidal magnetic field, $b_r^{2/1}/B_t$. The plasmas considered have magnetic equilibrium $q(a) \approx 1.7$ and electron density in the range $n_e = 1 - 2.5 \times 10^{19}$ m^{-3}.

First investigations reported in [24] showed that C VI decelerates as soon as the amplitude of the 2/1 RWM increases. The new flow data from O V, localized at a larger radius, also follows the same trend. The rotation braking is dictated by the stochastic force, associated with the presence of an ambipolar electric field in the plasma edge, as described by a 1D momentum transport model, that takes into account the NTV, the stochastic force and the friction force due to neutrals coming from the wall [24].

By combining C VI toroidal flow data with the O V data, information on the toroidal rotation profile can be gathered, since such ions are localized far apart across the radius, as suggested by the 1D collisional radiative impurity transport code [36]. The radial profiles of the toroidal flow, solutions of the 1D momentum transport model without and with externally applied magnetic field perturbations are plotted with green lines in figures 3 (*b*)–(*c*), respectively. The case with $b_r^{2/1}/B_t = 0.01\%$ represents a simulation without external magnetic field perturbation, instead, $b_r^{2/1}/B_t = 0.14\%$ with it. The corresponding mean C VI and O V toroidal flow velocities are indicated with circles on the same panels. A good agreement between the 1D momentum transport model and the experimental data has been obtained, confirming that the model, despite its simplicity, is able to capture the physical mechanisms which govern plasma rotation in the presence of a 2/1 RWM.

2.2. Plasma rotation in the presence of 2/1 tearing mode

In $q(a) > 2$ tokamak plasmas, a 2/1 rotating TM is present, which can transit from the fast rotation branch (some kHz) to the slow one (some Hz, as imposed by feedback control system), depending on the amplitude of the radial magnetic field at the resonant surface, as predicted theoretically in [44]. The plasma rotation is affected by the 2/1 TM dynamics when it rotates in the slow frequency branch, i.e. when it has a non-negligible amplitude.

An example of the interplay between toroidal rotation and 2/1 TM is reported in figure 4. This figure shows the time behaviour of the edge safety factor, the normalized radial magnetic field amplitude and the corresponding phase and frequency of the 2/1 TM and the O V toroidal flow.

As the magnetic equilibrium is approaching the $q(a) = 2$ resonance, the 2/1 TM increases in amplitude. In this case, it rotates in the slow frequency branch, at around 25 Hz, as shown in figure 4(*c*) and the O V toroidal rotation is nearly

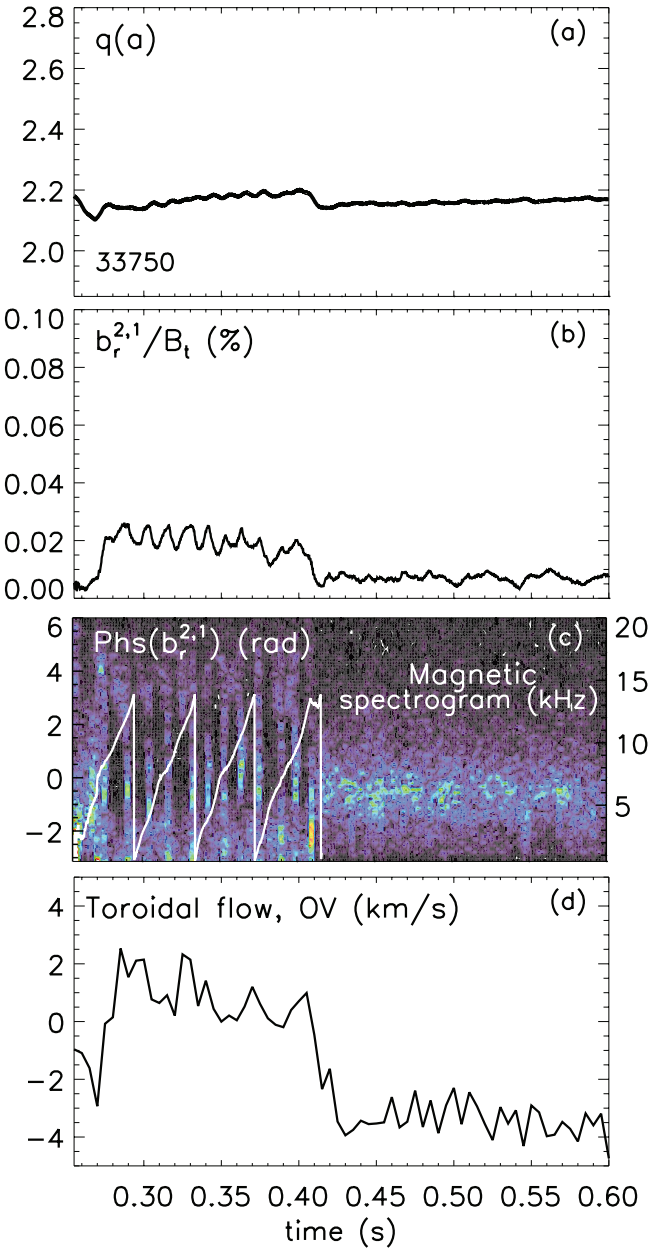

Figure 4. Time behaviour of (*a*) the edge safety factor, (*b*) the normalized radial magnetic field amplitude of the 2/1 TM, (*c*) the corresponding phase, together with the magnetic spectrogram which shows the mode behaviour in the fast frequency branch, and (*d*) O V toroidal flow.

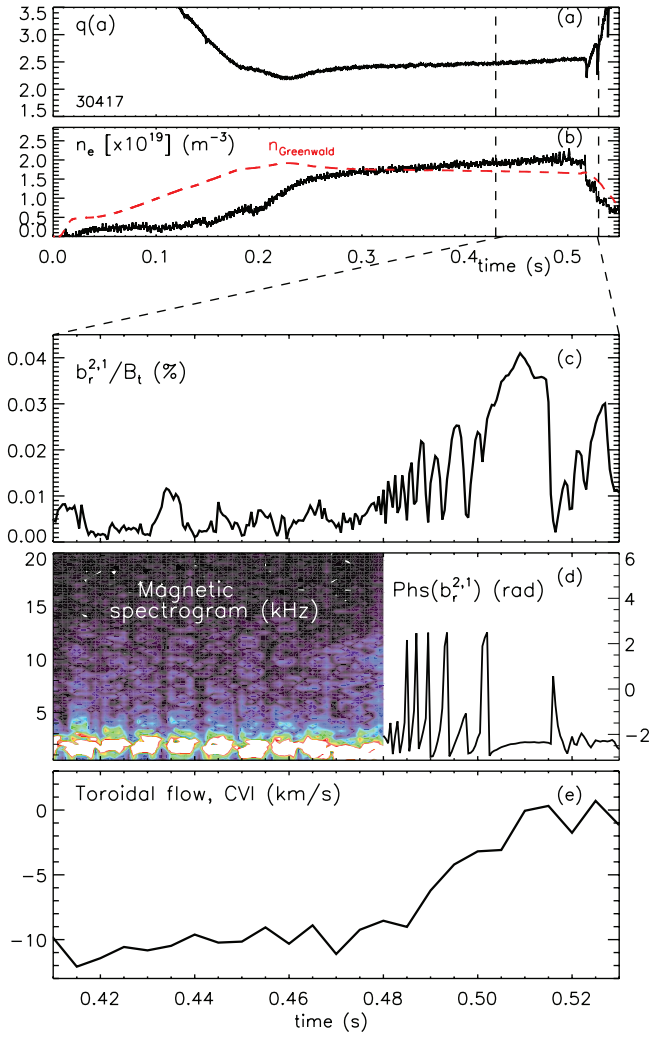

Figure 5. Time behaviour of (*a*) the edge safety factor, (*b*) electron density, in black, and calculated Greenwald density, in red, (*c*) the normalized radial magnetic field amplitude of the 2/1 TM, (*d*) the corresponding phase, together with the magnetic spectrogram, and (*e*) C VI toroidal flow.

1.5 km s^{-1} in co-I_p direction. As soon as the mode decreases in amplitude, probably due to modifications in the equilibrium profile, at around $t = 0.4$ s, it jumps into the fast rotation branch, rotating at 5 kHz, and the O V toroidal flow rotates in counter-I_p direction at 4 km s^{-1}. In this experiment, the electron magnetic torque, induced by the presence of a localized singular current in the vicinity of the 2/1 resistive layer [45, 46], is responsible for the change in the rotation direction.

Instead, in experiments at high electron density, near the Greenwald density limit, it has been observed that the plasma rotation always slows down and stops due to the presence of a locked 2/1 TM. In the experiment reported in figure 5, before $t = 0.48$ s, a 2/1 TM is rotating in the fast frequency branch, at $f = 2$ kHz, as shown in figure 5(*d*). As the plasma approaches the density limit, reported in red in figure 5(*b*), the 2/1 TM slows down and increases in amplitude, up to a time instant in which the toroidal rotation brakes, as shown in figure 5(*e*), and a disruption is triggered. Also in this case, the dynamic of plasma rotation, during mode locking phase, is mainly governed by the electromagnetic torque, whose amplitude is increased since the size of the 2/1 TM island is getting larger as approaching the density limit.

These $q(a) > 2$ experiments confirm the existence of a strong relation between the TM activity and plasma rotation in RFX-mod tokamak plasmas. A similar connection has been observed for the 2/1 RWM case, as described previously, even though the mechanisms governing the momentum transport are different.

3. Characterization of helical flow

As reported in the previous section, the 2/1 RWM in $q(a) < 2$ plasmas can be maintained at fixed amplitude by applying rotating 3D magnetic fields. In this kind of experiment, in

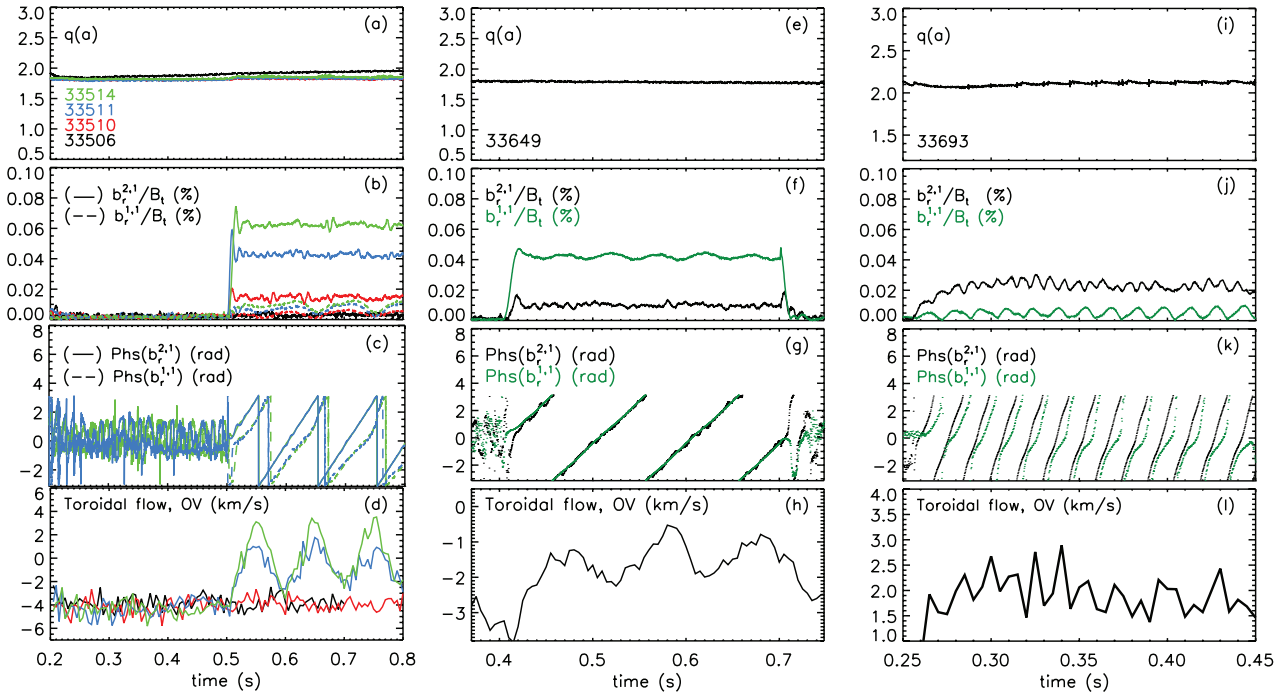

Figure 6. Time behaviour of (*a*)–(*e*)–(*i*) edge safety factor, (*b*)–(*f*)–(*j*) normalized radial magnetic field amplitude and (*c*)–(*g*)–(*k*) the corresponding phase of the 2/1 and 1/1 harmonics and (*d*)–(*h*)–(*l*) O V toroidal flow. On the left hand side: similar $q(a) < 2$ plasma experiments are shown in which 2/1 magnetic field perturbations at increasing amplitude (different colours) rotating at $f = 10$ Hz have been externally applied. The 2/1 RWM dynamic is represented with a solid line, the internal 1/1 kink mode dynamic with a dashed line. In the center: a $q(a) < 2$ plasma experiment is reported, in the presence of an externally applied 1/1 magnetic field perturbation rotating at $f = 10$ Hz. The 2/1 RWM dynamic is represented in black, the internal 1/1 kink mode dynamic in green. On the right hand side: a $q(a) > 2$ plasma experiment is shown in which a 2/1 magnetic field perturbation rotating at $f = 25$ Hz is externally applied. The 2/1 TM dynamic is represented in black, the internal 1/1 kink mode dynamic in green.

addition to a reduction of toroidal flow with increasing the 2/1 radial magnetic field amplitude, as shown in figure 3(*a*), oscillations in the plasma rotation measurements have been observed. In the following sections, we describe the experiments in which toroidal flow oscillations have been observed and discuss the argument for the presence of $m = 1$, $n = 1$ convective cells in the flow pattern.

3.1. Rotating 3D magnetic fields force toroidal flow oscillations

Figures 6(*a*)–(*d*) represents 4 $q(a) < 2$ pulses in which magnetic perturbations with 2/1 helicity and increasing amplitude, rotating at 10 Hz frequency, have been applied through the feedback control system. In particular, the figure shows the time behaviour of edge safety factor, the normalized radial magnetic field amplitude and the corresponding phase of the 2/1 RWM (solid line) and the internal 1/1 kink mode (dotted line), and the O V toroidal flow. Here, the colour code distinguishes different amplitudes of the applied perturbation. Note that, for simplicity, the temporal dynamics of the mode phases, reported in figure 6(*c*), have been represented only by the pulses highlighted in blue and in green.

In the presence of rotating 3D magnetic fields, the 2/1 RWM mode is kept at finite amplitude and rotates at 10 Hz, the same frequency imposed by magnetic feedback, as shown in figures 6(*b*)–(*c*). A phase shift between the target feedback harmonic and the externally applied magnetic field is present, which exerts an electromagnetic torque on the 2/1 RWM, forcing it into rotation [48, 49].

In these plasmas, a 1/1 magnetic field harmonic is induced by toroidal coupling, which resonates with the internal 1/1 kink mode. The internal 1/1 kink mode is thus affected by 3D magnetic fields. Its amplitude is lower than the 2/1 RWM amplitude, but it is finite, as shown in figure 6(*b*). The internal 1/1 kink mode rotates at the same frequency as the external perturbation when the amplitude of the 2/1 external magnetic field perturbation is larger than a threshold $b_r^{2,1}/B_t$, which is around 0.04%, as in the pulses highlighted in blue and green. Otherwise, the temporal dynamic behaviour of the 1/1 mode phase is similar to the behaviour without external magnetic field, which is shown in figure 6(*c*), before $t = 0.5$ s.

It is noteworthy that a helical deformation of magnetic surfaces associated with the internal 1/1 kink mode is observed in SXR data in the presence of 3D magnetic fields [26].

The external 3D magnetic field affects not only MHD modes but also toroidal rotation. Figure 6(*d*) shows that in these experiments, the O V toroidal rotation can either oscillate, as shown in blue and green, or stay constant, as shown in red, depending on the amplitude of the applied magnetic field. The O V toroidal flow oscillations appear for values of $b_r^{2,1}/B_t$ above 0.04%, which is the same threshold above which the internal 1/1 kink mode is maintained into rotation. Note that the frequency of the flow oscillations corresponds to the frequency of either the externally applied field or the MHD modes: the 2/1 RWM and the internal 1/1 kink mode.

Oscillations in O V toroidal flow are also induced in the presence of externally applied rotating magnetic fields with 1/1 helicity, as shown in figures 6(*e*)–(*h*). In this case the amplitude of the internal 1/1 kink mode is kept at finite amplitude and the mode rotates at 10 Hz, as reported in green in figures 6(*f*)–(*g*), respectively. Since a 2/1 sideband is induced by toroidal coupling, the 2/1 RWM, highlighted in black in the same panels, also has finite amplitude and rotates at the same frequency. As reported in figure 6(*h*), the O V toroidal flow oscillates at 10 Hz, the same frequency as the externally applied magnetic field.

Rotating 2/1 magnetic field perturbations have been applied through magnetic feedback also on plasma with $q(a) > 2$, presenting a 2/1 TM. Figures 6(*i*)–(*l*) represents an example. In particular, the figure shows the time behaviour of the edge safety factor, the normalized radial magnetic field amplitude and the corresponding phase of the 2/1 TM (in black) and the internal 1/1 kink mode (in green); the toroidal flow measurement from O V emission of a $q(a) = 2.1$ experiment where a 3D magnetic field rotating at 25 Hz has been externally applied. In this case, the 2/1 TM has a relatively large amplitude and therefore is forced by the magnetic feedback control system to rotate in the slow frequency branch, at 25 Hz. The toroidal flow oscillations are correlated with the 2/1 mode rotation, as shown in figure 6(*l*).

In summary, whenever the MHD mode is forced into slow rotation by magnetic feedback control (2/1 RWM or 2/1 TM and the internal 1/1 kink mode), toroidal flow oscillations can be observed. Although the examples reported here characterize the behaviour of O V toroidal flow, similar oscillations have been observed in data from different ions and also in the poloidal flow measurements, as will be discussed below.

3.2. Evidence of $m = 1$ and $n = 1$ convective cells in flow pattern

Measurements of different impurity spectral lines from C VI, C V, O V and C III, have been collected in $q(a) < 2$ plasmas and in the presence of a 2/1 RWM and the internal 1/1 kink mode, maintained at constant amplitude and rotating by means of externally applied 3D magnetic fields. Such measurements allow us to gather information on the effect of magnetic field perturbations on plasma rotation at different radial positions: C VI and C V in the core, and O V and C III near the plasma edge. Table 1 shows the radial localization of the different ion impurities, predicted by use of the 1D collisional radiative impurity transport code described in section 2.

Figures 7 (*a*)–(*d*) show the time behaviour of the edge safety factor and figures 7 (*e*)–(*h*) show the toroidal rotation measurements inferred from C VI, C V, O V and C III emission, respectively, in 4 similar pulses and in the presence of rotating 3D magnetic fields with 2/1 helicity. The dotted line superimposed on the toroidal flow data corresponds to the 2/1 radial magnetic field fluctuation. The 1/1 radial magnetic field fluctuation (not shown here) shows a time behaviour similar to that of the 2/1 RWM, since the 2/1 RWM and the internal 1/1 kink mode both rotate at the same frequency, as imposed by the magnetic feedback control system.

Table 1. Radial localization of the different ion impurities, calculated using the 1D collisional radiative impurity transport code described in section 2. B II, B IV flow data are not present in RFX-mod, but they are reported here since they have been simulated by the 2D flow modelling code, described in section 4.

Ion	Radial location (r/a)
C VI	0.35 ± 0.5
B V	0.47 ± 0.5
C V	0.56 ± 0.5
B IV	0.76 ± 0.5
O V	0.81 ± 0.5
C III	0.87 ± 0.5
B II	0.91 ± 0.5

Note that flow data from different impurities shares a common behaviour: the toroidal rotation oscillates at the same frequency as the externally applied rotating magnetic field perturbation, i.e. MHD modes. This suggests the presence of a $n = 1$ rotating structure in the flow pattern, as discussed below and as demonstrated in section 4.

In order to reconstruct the toroidal flow pattern, flow measurements in multiple toroidal locations would be required, but these are not available in RFX-mod passive Doppler spectroscopy diagnostics. The LOS geometry of the diagnostic is represented in figure 1 on the left. On the other hand, the assumption that the flow pattern is toroidally rotating can be exploited in order to sample it at different toroidal angles. Thus, the observation of the flow pattern in a single toroidal position for consecutive time frames is equivalent to the observation in multiple toroidal positions, at the same time frame. For this reason, the sole observation of a single full oscillation of the flow during one complete rotation of the external magnetic field perturbation is a signature of an $n = 1$ periodicity of the flow pattern.

Instead, the correlation of flow measurements from different ion emissions with magnetic data demonstrates the presence of a convective cell in the flow map. In fact, while C VI and C V toroidal flows show oscillations in phase with the magnetics, as shown in figures 7(*e*) and (*f*), O V and C III flows are in anti-phase, as in figures 7(*g*) and (*h*). Therefore, in the plasma center, the toroidal flow oscillates in one direction, but at the edge in the opposite direction.

Since the toroidal flow oscillates as the external magnetic field, i.e. MHD modes, and a radial inversion of the flow oscillations has been observed by correlating the toroidal flow and magnetic measurements, these evidences suggest the presence of a rotating $n = 1$ convective cell in the toroidal flow pattern.

Spectroscopic data are also available for the poloidal rotation in RFX-mod tokamak plasmas. Unlike the toroidal component, poloidal flow could be derived only from C V emission. In future RFX-mod tokamak operations, a doped pellet injector will be used in order to produce stronger emission lines allowing the study of the poloidal flow behaviour at different radial positions. C V poloidal flow measurements are available both in the high field side (HFS) and low field side (LFS) of the plasma, along LOS as plotted in figure 1, on the right.

The effect on poloidal rotation of an externally applied 3D magnetic field with 2/1 helicity, rotating at 10 Hz, is shown

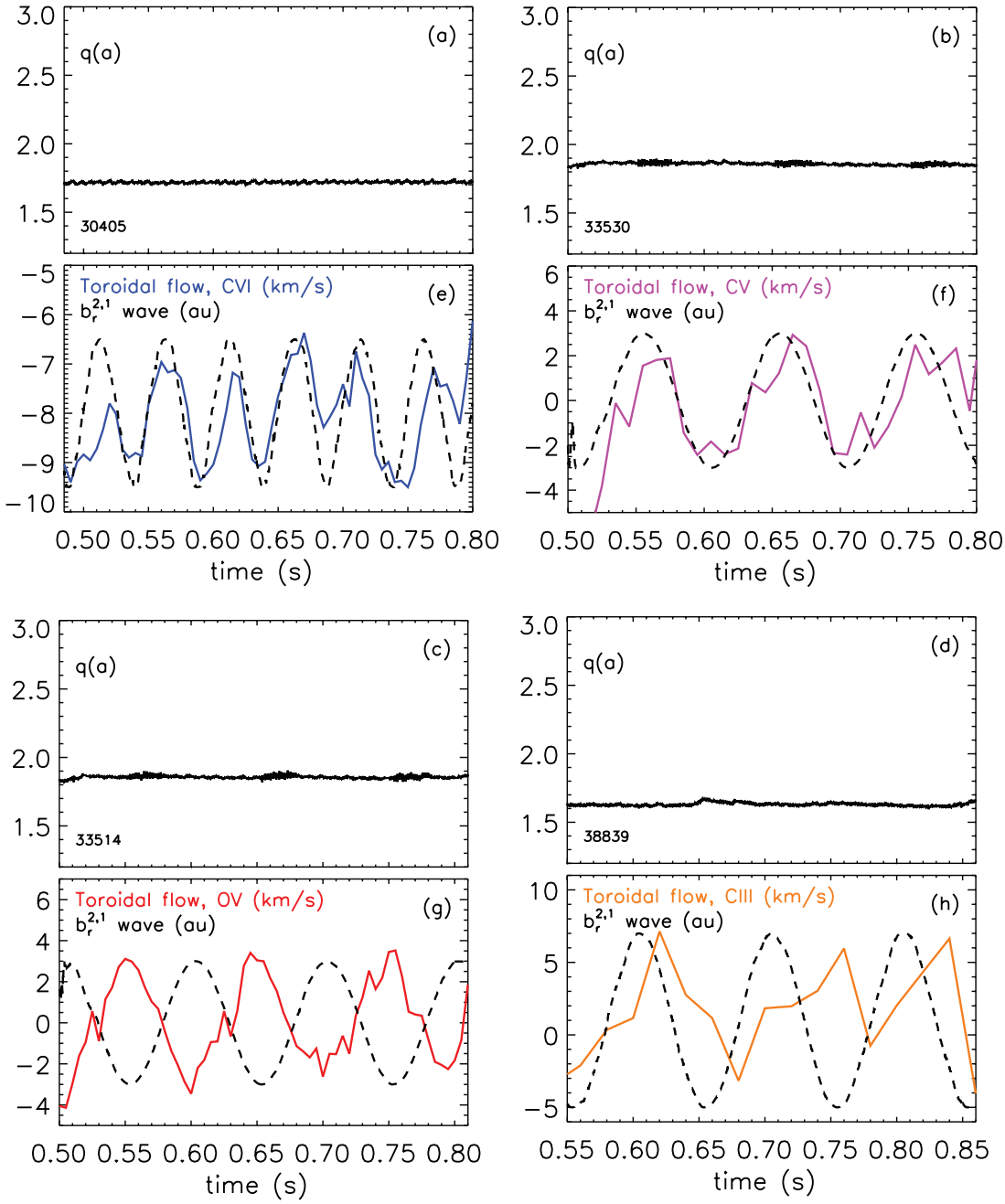

Figure 7. Time behaviour of (*a*)–(*d*) the edge safety factor and (*e*)–(*h*) C VI, C V, O V and C III toroidal flow, respectively. The dotted line corresponds to the 2/1 radial magnetic field fluctuation. In all the experiments, the 2/1 RWM and the internal 1/1 kink mode are kept at fixed amplitude and slowly rotating by an externally applied 2/1 magnetic field perturbation.

in figure 8. The amplitude of the external perturbation is not constant in time, as in the experiments reported previously but it increases during $t = 0.3$–0.55 s, and then decreases during $t = 0.55$–0.8 s. The 2/1 RWM and the internal 1/1 kink mode, whose dynamics are reported in figures 8(*b*)–(*c*), are affected by the external magnetic field: their amplitude follows the triangular shaped perturbation, and their frequency is the same as the external perturbation. As in the plasma experiments described above, the O V toroidal flow oscillates at the same frequency as the external perturbation, i.e. MHD modes, as shown in figure 8(*d*).

The time behaviour of poloidal flow is reported in figure 8(*e*), as measured by a LOS located in the HFS, in blue, and in the LFS, in red. Note that the time behaviour of these signals is quite similar.

In the presence of an oscillating $m = 1$ structure in the poloidal flow pattern, which can be represented as vertical arrows in a poloidal cross section, oscillations in phase should be detected by two LOS on opposite sides of the magnetic axis, as sketched in figure 9 on the left. Conversely, in the presence of an oscillating $m = 0$ structure, which implies a rotation around the poloidal angle, the two LOS should detect flow signals oscillating in anti-phase, as shown in figure 9 on the right.

Since the experimental time behaviour of the HFS and LFS poloidal flow signals are very similar in phase, an $m = 1$

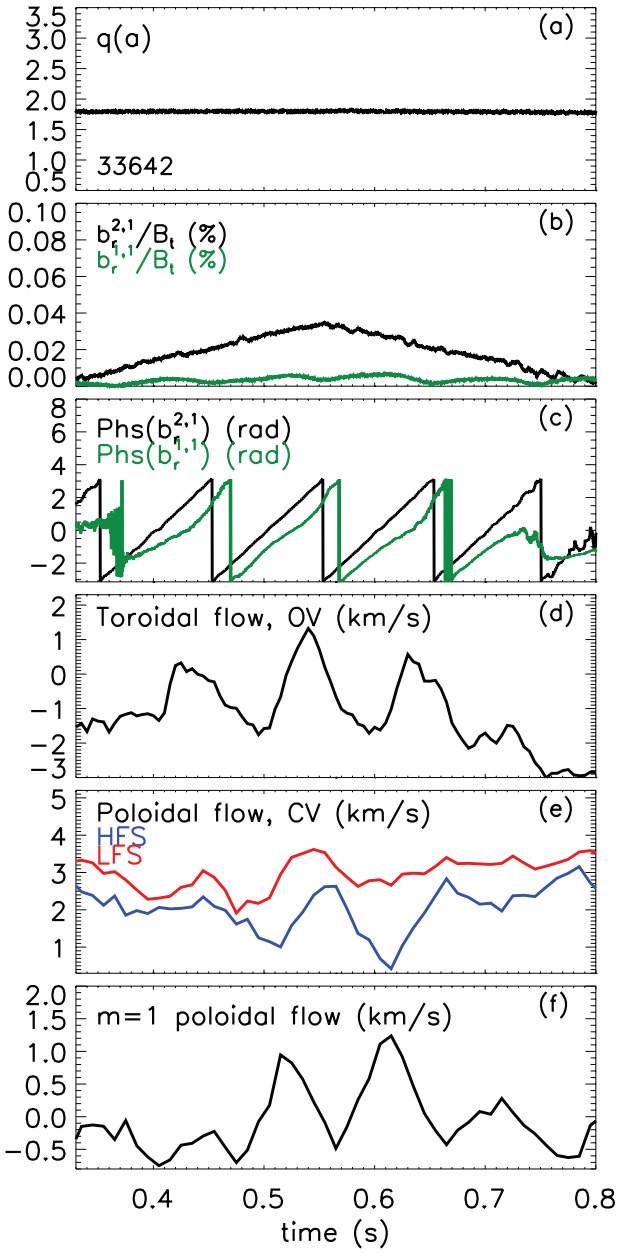

Figure 8. Time behaviour of (*a*) the edge safety factor, (*b*)–(*c*) the normalized radial magnetic field amplitude and the corresponding phase of the 2/1 RWM (in black) and internal 1/1 kink mode (in green), (*d*) O V toroidal flow, (*e*) C V poloidal flow as measured in the HFS (in blue) and in the LFS (in red) and (*f*) $m = 1$ poloidal flow component of a $q(a) < 2$ plasma experiment in which a 2/1 triangular shaped magnetic field perturbation rotating at 10 Hz is applied through the magnetic feedback control system.

structure in the poloidal flow map is present. In order to eliminate the even m components in the poloidal flow, the difference of the flow measurements reported in figure 8(*e*) has been calculated and this quantity is reported in figure 8(*f*). Despite the small amplitude of the oscillations, around 1 km s^{-1}, the time behaviour of such odd m contributions to the flow are correlated with the internal 1/1 kink mode dynamic. In contrast, the even m contributions do not show any correlation. This evidence reinforces the presence of an $m = 1$ convective cell.

Because $n = 1$ and $m = 1$ modulations have been observed at the same time in the rotation data, we can therefore claim that the plasma rotation is helically deformed. Such flow distortion has been observed in the presence of externally applied rotating perturbations since in this situation the internal 1/1 kink mode amplitude and the associated flux surface deformation is larger than that in standard plasmas, without externally applied magnetic field perturbations. Moreover, the 1/1 helical structure is rotating in front of the Doppler spectroscopic diagnostic, allowing measurement of the helical flow modulation. This is very similar to what has been observed in RFP configuration, both in RFX-mod and MST devices, where the helical flow is linked to the innermost resonant TM [37, 38, 47].

In order to prove that the observed flow oscillations are a signature of helical flow, a 2D flow modelling code has been developed. This is the topic of the next section.

4. Modelling of helical flow pattern

The existence of a helical dynamo velocity field associated with the helical deformation of the magnetic surfaces has been predicted by several codes [29–32]. Among them, the 3D, fully non-linear PIXIE3D code [30] solves the nonlinear visco-resistive 3D MHD model, whose equations in toroidal geometry are stated in [50], for example. The code has been benchmarked against Specyl code in [51]. It has been used in [50] to describe sawtooth mitigation in the presence of external 3D magnetic fields in tokamak plasmas and in [24] to understand the physical mechanisms ruling the momentum transport in the presence of 2/1 RWM.

Here, PIXIE3D code has been used to simulate the flow pattern, which has been given as input to a 2D flow modelling code. Such code calculates synthetic flow measurements by using PIXIE3D flow map, the ion emission profiles calculated by the 1D collisional radiative impurity transport code, as described in section 2, and a diagnostic geometry similar to that of the RFX-mod. This tool has allowed us to explain the nature of the flow oscillations experimentally observed.

In particular, PIXIE3D simulations considered in this work used on-axis Lundquist number $S = 3 \times 10^4$, Prandtl number $P = 3$, aspect ratio $R/a = 4$, initial axisymmetric equilibrium with $q(0) = 0.8$, $q(a) = 1.9$, and current density profile in the form $j_\phi = j_0(1 - (r/a)^2)^\nu$ where $\nu = q(a)/q(0) - 1$, as in [24]. A vacuum region between the plasma boundary ($r = a$), which ideally corresponds to the position of the graphite tiles in RFX-mod, and the wall ($r/a = 1.1$) is modelled by a region with large resistivity. The presence of a 2/1 3D magnetic field in PIXIE3D is modelled adding a fixed helical component with 2/1 helicity to the wall, which behaves as an ideal shell.

When applying such a 3D magnetic field, the dynamic of the internal 1/1 kink mode is also affected due to the toroidal coupling. Experimentally, the sawtooth period and its amplitude decrease and a stationary 1/1 helical equilibrium forms. The PIXIE3D code is able to describe such dynamics, as documented in [26].

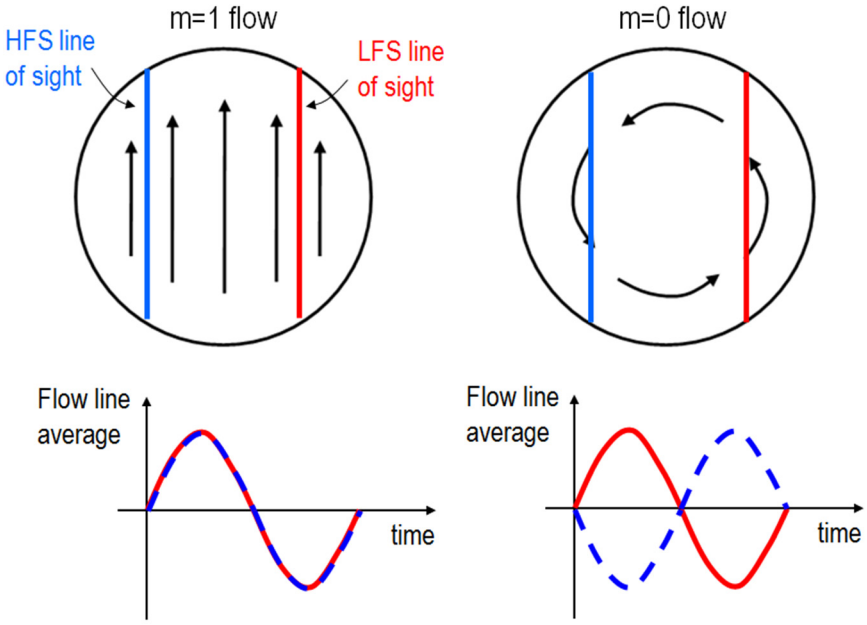

Figure 9. $m = 1$ and $m = 0$ (black arrows) flow pattern in the poloidal plane, on the left and the right, respectively, and the corresponding time behaviour of flow line average as detected by a LOS in the HFS (in blue) and in the LFS (in red).

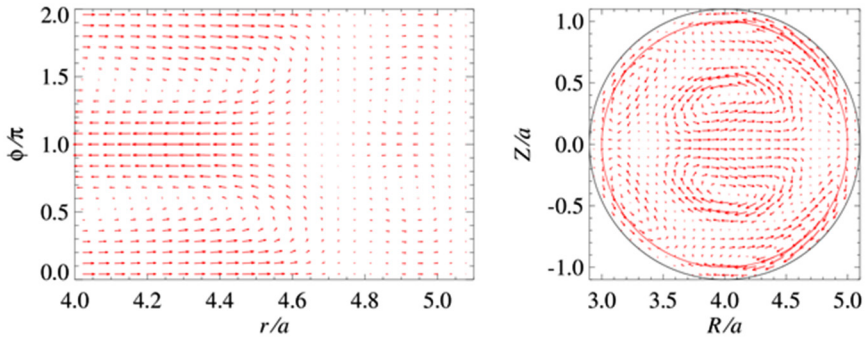

Figure 10. Toroidal (on the left) and poloidal (on the right) flow map from PIXIE3D RFX-mod tokamak simulation with $q(a) = 1.9$ in the presence of $b_r^{2/1}/B_t \approx 0.1\%$ magnetic field perturbation.

To highlight the effect of the 3D magnetic fields on the plasma rotation a 2/1 magnetic field perturbation with relatively large amplitude, of about $b_r^{2/1}/B_t \approx 0.1\%$, has been used in the code. Figure 10 represents the flow pattern in a toroidal (on the left) and poloidal (on the right) cross section, based on the outputs of the PIXIE3D simulation.

In the presence of an external 3D magnetic field, the code suggests the presence of $m = 1$, $n = 1$ convective cells in the flow pattern associated with the helical deformation of the internal 1/1 kink mode, which is mainly localized in the plasma core, and $m = 2$, $n = 1$ convective cells, at the position of the wall. The 2/1 convective cells appear since the 2/1 external kink develops and non-linearly saturates in the simulation with radial profile consistent with the 2/1 imposed helical boundary condition.

In the absence of an external 3D magnetic field, the $m = 2$, $n = 1$ convective cell does not appear in the flow map since no 2/1 helical boundary condition is applied. However, the code still foresees the presence of an $m = 1$, $n = 1$ convective cell in the flow map associated with the 1/1 internal kink mode. In particular, the 1/1 flow dynamic is dictated by the sawtooth behaviour. Close to the sawtooth crash, that is when the internal 1/1 kink mode has the largest amplitude, the 1/1 flow pattern is similar to that in the presence of an external 3D magnetic field. Then the 1/1 flow pattern disappears after the sawtooth crash and it appears again close to the next one.

In RFX-mod experiments without externally applied magnetic field perturbations, the presence of these 1/1 convective cells could not be detected by the Doppler spectroscopic diagnostic since the time integration of the rotation signals is larger than the sawtooth period. However, the application of the 3D magnetic fields allows the amplitude of the internal 1/1 kink mode and the corresponding convective cell to increase, and the sawtooth intermittent behaviour is replaced by a stationary 1/1 helical equilibrium [26]. In such condition, we are able to drive the rotation of the helical core, maintaining it into rotation at the desired frequency, and the Doppler spectroscopic diagnostic is able to measure the flow modulation quite accurately, as described in the previous section.

In order to model the flow pattern and to reconstruct the measurements in the presence of external 3D magnetic fields,

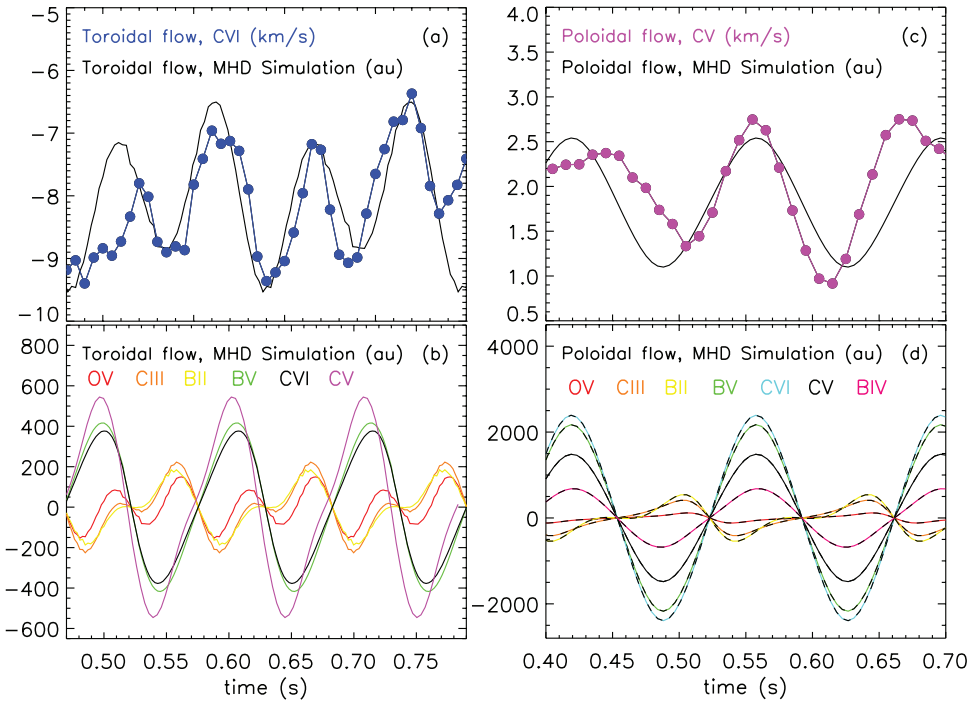

Figure 11. (*a*) Time behaviour of C VI toroidal from 30405 experiment (blue dots) and from PIXIE3D simulation (black line), (*b*) time behaviour of toroidal flow of multiple ion species, predicted by PIXIE3D code. The signals correspond to a LOS in the poloidal plasma cross section with impact parameter $\rho/a = 0.4$. (*c*) Time behaviour of C V poloidal flow from 33642 experiment (magenta dots) and from PIXIE3D simulation (black line) (*d*) time behaviour of poloidal flow of multiple ion species, predicted by PIXIE3D code. The signals correspond to two lines of sight, with impact parameter $\rho/a = 0.2$, located on opposite sides of the magnetic axis. The LOS in the HFS is represented with a solid line, the LOS in the LFS with a dashed line. Different colours have been used to distinguish flow from different ions emission.

as mentioned before, a 2D flow modelling code has been developed. The 2D flow modelling code divides the PIXIE3D flow map in fine elements, i.e. cells. The cell grids used, together with the LOS geometry, are shown in figure 1.

For each cell, a vector has been assigned. The components of the vector correspond to the toroidal and poloidal flow component, $\mathbf{v}(\mathbf{x})$. For each cell, a value of ion emissivity, ξ^{ion} is also ascribed. The flow measured along a LOS, for a certain ion can be written as $\langle v^{\mathrm{ion}}_{\mathrm{LOS}}\rangle = \int_{\mathrm{LOS}} \xi^{\mathrm{ion}}(\mathbf{x})\mathbf{v}(\mathbf{x})\cdot \mathrm{d}\mathbf{x} / \int_{\mathrm{LOS}} \xi^{\mathrm{ion}}(\mathbf{x})\mathrm{d}\mathbf{x}$. To calculate the mean flow along the LOS, the following expression has been used $\langle v^{\mathrm{ion}}_{\mathrm{LOS}}\rangle \cong \sum_{i-\mathrm{cell}} \xi^{\mathrm{ion}}_i(\mathbf{v}\cdot\widehat{\mathrm{LOS}})_i l_i / \sum_{i-\mathrm{cell}} \xi^{\mathrm{ion}}_i l_i$, where l_i represents the length of the LOS inside the i-cell.

The time evolution of the plasma flow has been reconstructed by simply rotating the LOS when calculating the toroidal flow measurements, instead considering sections at different toroidal angles for the poloidal ones.

Figure 11(*a*) shows a comparison between the reconstructed C VI toroidal flow, indicated with a black line, and the experimental one, indicated with blue dots, for a LOS with impact parameter $\rho/a = 0.4$. This LOS is indicated in red in figure 1, on the left. Oscillations can be detected in the synthetic flow measurement and they are due to the presence of a $n = 1$ structure in the PIXIE3D flow pattern. This $n = 1$ structure is associated with the magnetic deformation due to the internal 1/1 kink mode. These oscillations match with the experimentally observed oscillations. This proves that the experimental flow oscillations are induced by the internal 1/1 kink mode which is forced to rotate by the external magnetic field.

Moreover, synthetic flow measurements, simulated along the same LOS, have been calculated from the emission of different ion species, whose radial location is reported in table 1. The time behaviour of these synthetic measurements is plotted in figure 11(*b*) in different colors. The PIXIE3D code foresees that the toroidal flow in the core oscillates in opposite phase with respect to the one at the edge. This behaviour is similar to what has been observed experimentally: the toroidal flow deduced from C V and C VI, ions located in the core, oscillates in phase with the magnetics, conversely, the toroidal flow from O V and C III, ions located at the edge, oscillates in antiphase, as shown in figure 7. Based on the agreement between the 2D flow modelling code predictions and the experimental flow data, we can conclude that an $n = 1$ convective cell is present in the toroidal flow map.

A similar analysis has been carried out for the poloidal component of plasma rotation. Figure 11(*c*) shows the time behaviour of the synthetic poloidal C V flow, plotted with a black line, and the experimental data, indicated with magenta dots, as detected by a LOS located in the HFS, with impact parameter $\rho = 0.2$. Such LOS is shown in blue in figure 1, on the right. A good agreement has been obtained between the experimental and synthetic flow behaviour, demonstrating that the poloidal flow modulation is linked to the dynamic of the internal 1/1 kink mode.

In addition to this, synthetic poloidal flow measurements have been reconstructed for a LOS in the LFS with the same impact parameter as that in the HFS. This LOS is highlighted in red in figure 1 on the right. The time behaviour of HFS and

LFS synthetic flow measurements are shown in figure 11(*d*) with solid and dashed lines, respectively. The different colours in the figure represent the results for different ion species.

Regardless of the ion species analysed, HFS poloidal flow has the same time behaviour as in the LFS. This is consistent with the experimental data reported in figure 8(*e*), leading to the conclusion that an $m = 1$ component is present in the experimental flow pattern.

As it has been observed in the synthetic toroidal flow measurements from different ion species, the poloidal flow in the core oscillates with opposite phase with respect to the edge, as reported in figure 11(*d*). Since only poloidal C V flow data are currently available in RFX-mod, a direct comparison of flow behaviour from different ions cannot be performed. The 2D flow modelling code suggests that C VI and B IV flow oscillations have larger amplitude with respect to edge ions, such as O V, C III or B II. Measurements for these different ions in future RFX-mod experiments will allow us to further confirm the presence of an $m = 1$ convective cell.

The good agreement between the synthetic and experimental flow behaviour confirms the assumption that the flow pattern in the presence of 3D magnetic field perturbations is associated with rotating convective cells with $m = 1$, $n = 1$ helicity.

It is worth mentioning that the comparison between the synthetic flow measurements and the experimental flow measurements can be done presently only on a qualitative basis. Indeed, the present version of PIXIE3D neglects any momentum source in the momentum balance equation, both in the toroidal and poloidal directions. Furthermore, the code assumes the same phase for all the modes, therefore, the mean electromagnetic torque is null as well. These assumptions imply that the mean flow is zero in the present version of the code. This prevents us from directly comparing the mean flow behaviour predicted by the code varying the plasma parameters and the experimental data, shown in figure 2. As mentioned in [50], a recent an upgrade of the present version of PIXIE3D code has been performed which includes a toroidal momentum source in the momentum balance equation. A detailed investigation of this issue is beyond the scope of this work and will be addressed in a future paper.

5. Conclusions

In this work, the intrinsic rotation in RFX-mod tokamak plasma has been characterized, analysing Doppler spectroscopic diagnostic data in plasmas with and without 3D magnetic field perturbations.

Without magnetic field perturbations, toroidal rotation depends strongly on the edge safety factor, but not on plasma electron density. This is different from Alcator-C Mod results which show a flow inversion above a threshold value of electron density [42].

In the presence of externally applied rotating 3D magnetic fields which keep 2/1 RWMs at finite amplitudes, along with a reduction of toroidal rotation [24], oscillations have been observed in rotation measurements. Generally, flow oscillations have been detected in plasmas with $q(a) < 2$ and $q(a) > 2$. In this paper, the experimental characterization of these oscillations and the corresponding modelling have been presented for plasmas with $q(a) < 2$.

Toroidal flow oscillations have been observed in plasmas with $b_r^{2/1}/B_t$ above a threshold value, around 0.04%, where the internal 1/1 kink mode is kept rotating by the external 3D magnetic field and a helical equilibrium with 1/1 helicity forms [26]. The oscillations appear both in the core, as shown by C V and C VI flow data, and at the edge, as indicated by O V and C III flow data. In particular, the toroidal flow oscillates in phase with the magnetics, i.e. MHD modes, in the core. Conversely, it oscillates in anti-phase, at the edge. This suggests the presence of an $n = 1$ convective cell in the toroidal flow map.

The poloidal component of plasma rotation also exhibits an oscillatory behaviour in these experiments. In particular, poloidal flow measurements along LOS on opposite sides of the magnetic axis are acquired by the Doppler spectroscopic diagnostic, allowing the study of plasma rotation in the plasma HFS and LFS. These poloidal flow signals show the same temporal dynamics and by extracting the $m = 1$ poloidal flow component, which is obtained by taking their difference, oscillations can be observed. These have a small amplitude, of about 1 km s^{-1}, and are correlated with the internal 1/1 kink mode dynamic. These evidences suggest the presence of an $m = 1$ convective cell in the poloidal flow pattern.

The existence of a helical dynamo velocity field associated with the helical deformation of the flux surfaces has been predicted in several codes [29–32]. In particular, the 3D, fully non-linear PIXIE3D code [30], which has been validated against RFX-mod tokamak data in [24, 26, 35], has been used in this work to study the origin of the oscillations in flow measurements. For this purpose, a 2D flow modelling code has been developed that can reconstruct synthetic flow measurements from the PIXIE3D code flow map, a diagnostic with a geometry similar to the experimental one and ion emission profiles as obtained by the 1D collisional radiative impurity transport code [36].

A good agreement between synthetic flow measurements and experimental results has been obtained, on both the toroidal and poloidal flow components, confirming that the flow oscillations are associated with the presence of $m = 1$, $n = 1$ convective cells in the flow pattern. Therefore, the oscillations in the rotation data are the signature of a helical flow.

In addition, in the presence of externally applied 3D magnetic fields, SXR core data shows the presence of a 1/1 stationary helical equilibrium [26]. The evidences imply that a helical equilibrium sustained by the dynamo mechanism can exist in RFX-mod tokamak plasmas [30, 33, 34]. Helical equilibria have been observed in the same device when operated as a RFP exploring high plasma current regimes [37, 47] and in the MST RFP experiment [38]. In these RPF plasmas, helical equilibria are sustained by the innermost resonant TM. Conversely, in the tokamak experiments analysed here, they are associated with the internal 1/1 kink mode.

The dynamo mechanism plays a role in sustaining helical equilibria not only in high current RFP and in low-β RFX-mod tokamak plasmas, but also in high-β DIII-D tokamaks hybrid

operations [34, 39]. In DIII-D hybrid plasmas, the observed peaking of the toroidal current density associated with a redistribution of the current profile (or poloidal flux, hence the name flux-pumping [52]), has been explained recently as a self-organization process of the current profile, in which a stationary marginal core interchange mode maintains a helical equilibrium through the dynamo mechanism [32].

The analysis presented in this work, which demonstrates the presence of a helical flow pattern for the first time in a tokamak plasma, can be used therefore to validate the MHD dynamo model [34] in which the dynamo or flux pumping mechanism is responsible for the redistribution of the current profile and for sustaining helical equilibria in fusion plasmas.

Acknowledgments

The author is grateful to L. Chacón for providing the PIXIE3D code and valuable comments and Teruo Tamano for improving the manuscript. This work has been carried out within the framework of the EUROfusion Consortium and has received funding from the Euratom research and training programme 2014-2018 under grant agreement No 633053. The views and opinions expressed herein do not necessarily reflect those of the European Commission. This project has also received funding from the RCUK Energy Programme (grant number EP/I501045). To obtain further information on the data and models underlying this paper please contact PublicationsManager@ccfe.ac.uk.

References

[1] La Haye R.J. *et al* 2010 *Phys. Plasmas* **17** 056110
[2] Chu M.S. and Okabayashi M. 2010 *Plasma Phys. Control. Fusion* **52** 123001
[3] Fitzpatrick R. 1998 *Phys. Plasmas* **5** 3325
[4] Burrell K.H. 1998 *Science* **281** 1816
[5] Zanca P. *et al* 2012 *Plasma Phys. Control. Fusion* **54** 094004
[6] Evans T.E. *et al* 2004 *Phys. Rev. Lett.* **92** 235003
[7] Frassinetti L. *et al* 2010 *Nucl. Fusion* **50** 035005
[8] Schmitz O. *et al* 2009 *J. Nucl. Mater.* **390–1** 330
[9] Lehnen M. *et al* 2008 *Phys. Rev. Lett.* **100** 255003
[10] Callen J.D. *et al* 2011 *Nucl. Fusion* **51** 094026
[11] Zohm H. *et al* 1990 *Europhys. Lett.* **11** 745
[12] Snipes J.A. *et al* 1990 *Nucl. Fusion* **30** 205
[13] Scoville J.T. *et al* 1991 *Nucl. Fusion* **31** 875
[14] Taylor E.D. *et al* 2002 *Phys. Plasmas* **9** 3938
[15] Evans T. *et al* 2008 *Nucl. Fusion* **48** 024002
[16] De Bock M.F.M. *et al* 2008 *Nucl. Fusion* **48** 015007
[17] Zhu W. *et al* 2006 *Phys. Rev. Lett.* **96** 225002
[18] Garofalo A.M. *et al* 2008 *Phys. Rev. Lett.* **101** 195005
[19] Frassinetti L. *et al* 2015 *Nucl. Fusion* **55** 112003
[20] Sonato P. *et al* 2003 *Fusion Eng. Des.* **66** 161
[21] Martin P. *et al* 2011 *Nucl. Fusion* **51** 094023
[22] Baruzzo M. *et al* 2012 *Nucl. Fusion* **52** 103001
[23] Zanca P. *et al* 2015 *Nucl. Fusion* **55** 043020
[24] Piron L. *et al* 2013 *Nucl. Fusion* **53** 113022
[25] Cooper W.A. *et al* 2010 *Phys. Rev. Lett.* **105** 035003
[26] Piron C. *et al* 2016 *Nucl. Fusion* **56** 106012
[27] Lorenzini R. *et al* 2009 *Nat. Phys.* **5** 570
[28] Bergerson W.F. *et al* 2011 *Phys. Rev. Lett.* **107** 255001
[29] Bonfiglio D. *et al* 2005 *Phys. Rev. Lett.* **94** 145001
[30] Chacón L. *et al* 2008 *Phys. Plasmas* **15** 056103
[31] King J.R. *et al* 2012 *Phys. Plasmas* **19** 055905
[32] Jardin S.C. *et al* 2015 *Phys. Rev. Lett.* **115** 215001
[33] Cappello S. *et al* 2011 *Nucl. Fusion* **51** 103012
[34] Piovesan P. *et al* 2016 Role of MHD dynamo in the formation of 3D equilibria in fusion plasmas *Nucl. Fusion* submitted
[35] Bonfiglio L. *et al* 2015 *Plasma Phys. Control. Fusion* **57** 044001
[36] Carraro L. *et al* 2000 *Plasma Phys. Control. Fusion* **42** 731
[37] Bonomo F. *et al* 2011 *Nucl. Fusion* **51** 123007
[38] Piovesan P. *et al* 2004 *Phys. Rev. Lett.* **93** 235001
[39] Luce T.C. *et al* 2014 *Nucl. Fusion* **54** 013015
[40] Scarabosio A. *et al* 2006 *Plasma Phys. Control. Fusion* **48** 663
[41] Rice J.E. *et al* 2011 *Nucl. Fusion* **51** 083005
[42] Rice J.E. *et al* 2016 *Plasma Phys. Control. Fusion* **58** 083001
[43] Helander P. and Sigmar D.J. 2000 *Collisional Transport in Magnetized Plasmas* (Cambridge: Cambridge University Press)
[44] Fitzpatrick R. 1999 *Phys. Plasmas* **6** 1168
[45] Nave M.F. *et al* 1990 *Nucl. Fusion* **30** 2575
[46] Yokoyama M. *et al* 1996 *Nucl. Fusion* **36** 1307
[47] Piovesan P. *et al* 2011 *Plasma Phys. Control. Fusion* **53** 084005
[48] Zanca P. *et al* 2007 *Nucl. Fusion* **47** 1425
[49] Piron L. *et al* 2010 *Nucl. Fusion* **50** 115011
[50] Bonfiglio L. *et al* 2017 *Plasma Phys. Control. Fusion* **59** 014032
[51] Bonfiglio D. *et al* 2010 *Phys. Plasmas* **17** 082501
[52] Petty C.C. *et al* 2009 *Phys. Rev. Lett.* **102** 045005